Cell and Tissue Research (2019) 378:499–511
https://doi.org/10.1007/s00441-019-03063-1

REGULAR ARTICLE

Autophagy in periodontal ligament fibroblasts under biomechanical loading

Svenja Memmert[1,2] · Anna Damanaki[3] · Beatrice Weykopf[4,5] · Birgit Rath-Deschner[1] · Marjan Nokhbehsaim[2] · Werner Götz[1] · Lina Gölz[6,7] · Andreas Till[8] · James Deschner[3] · Andreas Jäger[1]

Received: 18 December 2018 / Accepted: 1 July 2019 / Published online: 27 July 2019
© Springer-Verlag GmbH Germany, part of Springer Nature 2019

Abstract

Autophagy (cellular self-consumption) is an adaptive stress response and an important aspect of adaption to mechanical loading. If mechanical forces are associated with autophagy regulation in periodontal ligament (PDL) fibroblasts is still unknown. The aim of this study was to analyze the influence of force magnitude on autophagy regulation and subsequently on cell death in human PDL fibroblasts. Autophagy-associated genes were analyzed with a specific PrimePCR assay after 24 h of stimulation with high (STSH) and low magnitudes (STSL) of static tensile strain applied to PDL fibroblasts. Based on the results, targets were selected for further real-time PCR analysis. The autophagic flux was assessed by immunoblotting for autophagy marker microtubule-associated protein 1, light chain 3, and by autophagosome staining. Cell death was determined by TUNEL assay and Cell Death Detection ELISA^{PLUS}. Autophagy was induced pharmacologically by rapamycin and inhibited by chloroquine. For statistical analysis, the Kruskal Wallis test followed by the post-hoc Dunnett's test was used. Static tensile strain had regulatory effects on mRNA expression of multiple autophagy-associated targets. Stimulation with STSH induced mRNA expression changes in more autophagy-associated targets than STSL. The autophagic flux was induced by STSH while STSL had no significant effect on autophagosome formation. Furthermore, autophagy inhibition led to increased cell death. Low magnitudes of tensile strain seem to have cell-protective properties. Taken together, our findings provide novel insights about autophagy regulation by biomechanical loading in human PDL fibroblasts. Our results suggest a gradual response of autophagy to static tensile strain in human PDL fibroblasts.

Keywords Periodontal ligament · Autophagy · Biomechanical loading · Orthodontic tooth movement · Cell death

Introduction

One of the guiding principles of orthodontic treatment is to move teeth without damaging the involved tissues. In this context, a key issue for prevention is the applied force. The attempt to identify an ideal force for orthodontic tooth movement has been undertaken by many studies (Krishnan et al. 2015). A periodontal overload leads to an increased rate of cell death of periodontal ligament (PDL) fibroblasts whereas minimal forces may be too small to initiate tooth movement, thus

✉ Svenja Memmert
svenja.memmert@ukb.uni-bonn.de

[1] Department of Orthodontics, Center of Dento-Maxillo-Facial Medicine, University of Bonn Medical Center, Welschnonnenstr. 17, 53111 Bonn, Germany

[2] Section of Experimental Dento-Maxillo-Facial Medicine, Center of Dento-Maxillo-Facial Medicine, University of Bonn Medical Center, Bonn, Germany

[3] Department of Periodontology and Operative Dentistry, University Medical Center of the Johannes Gutenberg University, Mainz, Germany

[4] Precision Neurology Program, Harvard Medical School and Brigham & Women's Hospital, Boston, MA, USA

[5] Advanced Center for Parkinson's Disease Research of Harvard Medical School and Brigham & Women's Hospital, Boston, MA, USA

[6] Department of Orthodontics and Orofacial Orthopedics, University of Erlangen, Erlangen, Germany

[7] Institute of Human Genetics, University Hospital of Bonn, Bonn, Germany

[8] Institute of Reconstructive Neurobiology, Life & Brain Center, University of Bonn Medical Center, Bonn, Germany

both approaches result in a decelerated orthodontic treatment (Marchesan et al. 2011).

Physiologically, PDL fibroblasts are subjected to biomechanical forces during masticatory movements and orchestrate the subsequent adaption processes in the periodontium. A moderate periodontal loading has been shown to be an important factor in periodontal tissue homeostasis and to induce cell-protective signaling pathways (Deschner et al. 2012). On the other side, periodontal overload has been connected to an increased incidence of cell death in periodontal cells and tissues by multiple studies (Wu et al. 2016; Xu et al. 2011; Zhao et al. 2017). A mechanism underlying the turnaround might be autophagy, a highly-conserved process of adaption that helps to preserve cellular homeostasis and adapt to intrinsic and extrinsic insults, including malnutrition as well as mechanical, oxidative or inflammatory cell stresses (King 2012; Kroemer et al. 2010; Ma et al. 2013).

Autophagy (i.e., lysosomal self-consumption) is induced as an adaptive response under stressful conditions. It can either secure sell survival or trigger cell death dependent on the stress threshold (Mariño et al. 2014). Therefore, autophagy often precedes cell death (Mariño et al. 2014). Moreover, autophagy mediates lysosomal degradation of misfolded proteins, non-functional organelles, and intracellular pathogens (Glick et al. 2010). In general, autophagy comprises four phases: initiation, elongation of the autophagosome, its maturation, and degradation (Salabei and Hill 2015). Since multiple pathways are involved, autophagy regulation is complex. However, a special focus on the molecular control of autophagy lies on autophagy-related genes (ATGs), especially the molecules beclin-1 and the microtubule-associated protein 1, light chain 3 (LC3) (Huang and Klionsky 2002; Mizushima and Komatsu 2011; Wesselborg and Stork 2015). Post-translational modifications allow for rapid adaption, while a delayed and more permanent reaction takes place through transcriptional changes in an attempt to preserve or re-establish homeostasis (Pietrocola et al. 2013). Pharmacologically, autophagy can be induced by rapamycin or inhibited by chloroquine (Klionsky et al. 2016; Li et al. 2013; Noda and Ohsumi 1998; Towers and Thorburn 2016).

Mechanical stress is one of numerous conditions that have been reported to trigger autophagy. Mostly, autophagy as a part of mechanical adaption has been analyzed in specialized mechanosensitive cells such as osteoblasts and endothelial cells which need to adapt to their physical environment and reorganize their cytoskeleton to maintain functionality (King 2012). First, hints that autophagy could be important for mechanical adaptation in the periodontium were given by Nakamura and colleagues (Nakamura et al. 1984). In their study, they analyzed periodontal tissues of Wistar rats after 24 h of tooth movement by electron microscopy. They reported that vacuoles, which sometimes were fused with lysosomes and contained parts of other cellular organelles, were found inside osteoblasts as well as fibroblasts in the periodontium after tooth movement. These vacuoles were therefore identified as autophagosomes and autophagolysosomes. Furthermore, mechanically induced cell death was observed after 72 h of tooth movement (Nakamura et al. 1984). Autophagy might therefore be an important aspect of adaption to periodontal loading, but how mechanical forces, like static tensile strain, are involved in autophagy regulation of PDL fibroblasts is still unknown. Therefore, it is crucial to study the underlying mechanisms induced by biomechanical loading in PDL fibroblasts as key players in mechanical adaption in the course of orthodontic tooth movement. The aim of this study was to analyze the influence of force magnitude on autophagy regulation and consequently cell death in human PDL fibroblasts.

Materials and methods

Isolation and characterization of PDL fibroblasts

PDL cells were taken from periodontally healthy donors (mean age 14.38 years, min/max 11/19 years) after the approval of the Ethics Committee of the University of Bonn was given (#117/15). Patients or their legal guardians provided written informed consent before PDL cells were harvested from teeth extracted for orthodontic reasons as described elsewhere (Basdra and Komposch 1997; Mariotti and Cochran 1990). In brief, the medial part of the tooth root served as cell source before PDL cells were cultured in Dulbecco's minimal essential medium (DMEM, Invitrogen, Karlsruhe, Germany) supplemented with 10% fetal bovine serum (FBS, Invitrogen), 100 units/mL penicillin and 100 μg/ml streptomycin (Invitrogen) at 37 °C in a humidified atmosphere of 5% CO_2. Phenotyping for known specific markers, i.e., alkaline phosphatase, osteocalcin, periostin, and S100A4, was performed at the third passage. For experiments, PDL cells from the third to fifth passages were used in six-well plates (50,000 cells/well) and grown to 80% confluence (Basdra and Komposch 1997). One day prior to stimulation, the FBS concentration was reduced to 1%.

Cell stimulation

In order to apply biomechanical loading of various magnitudes, cells were seeded on BioFlex-II-culture plates (Flexcell International, Hillborough, NC, USA) and inserted into a special straining device, developed at the University of Bonn (Deschner et al. 2012). Static tensile strain of low (3%, STSL) and high magnitudes (20%, STSH) was applied to the cells for 4 h and 24 h. These force magnitudes were found to

be realistic compared to the strain subjected to the periodontal ligament in the course of orthodontic tooth movement, by chewing or grinding (Natali et al. 2004).

Analysis of gene expression

Adaptive stress responses such as autophagy execution take place in two phases. Within minutes or hours post-translational protein modifications allow for a rapid adaption to the new situation. A delayed reaction to a new environment is facilitated by changes on transcriptional level as an attempt to preserve or re-establish homeostasis (Pietrocola et al. 2013). Therefore, the expression of autophagy-associated genes was analyzed with a specific PrimePCR™ Assay (Autophagy (SAB Target List) H96, Bio-Rad Laboratories, Munich, Germany) after 24 h of biomechanical loading. A list of all genes covered by this assay is available at the manufacturer's website (http://www.bio-rad.com/de-de/prime-pcr-assays/predesigned-plate/sybrgreen-autophagy-sab-target-list-h96). PDL cells of three donors were exposed to STSL, STSH, or left untreated for 24 h. Total RNA was extracted with a commercially available RNA extraction kit (RNeasy Protect Minikit, Qiagen, Hilden, Germany) and 1 μg of RNA was reverse-transcribed with the iScript™ Select cDNA Synthesis Kit (Bio-Rad Laboratories). Real-time polymerase chain reaction (RT-PCR) was conducted with pooled cDNA of the three donors and as instructed by the manufacturer in an iCycler iQ5 Detection System (Bio-Rad Laboratories). Data normalization was done according to the manufacturer's instruction with three reference genes (glyceraldehyde-3-phosphate dehydrogenase (GAPDH), hypoxanthine phosphoribosyltransferase 1 (HPRT1), TATA box binding protein (TRP)) for comparative ΔΔ-CT analysis with the Software CFX-Manager (Bio-Rad Laboratories), provided by the manufacturer.

Based on the results of the PrimePCR™ Assay, target genes were selected for further analysis. The assessment of mRNA expression changes of these targets was performed with PDL fibroblasts of three donors. One microliter of cDNA (corresponding to 1 μg of total RNA) was used in a 25-μl reaction mixture containing 2.5 μl respective QuantiTect Primer Assay (Qiagen), 12.5 μl QuantiTect SYBR Green Master Mix (Qiagen), and 9 μl of nuclease-free water. The RT-PCR protocol included a heating phase at 95 °C for 5 min to activate the enzyme, 40 cycles including a denaturation step at 95 °C for 10 s, and a combined annealing/extension step at 60 °C for 30 s per cycle. The reference gene GAPDH was applied for normalization.

Autophagy detection

In order to quantify steady-state autophagy levels, the relation of the active form of LC3 (LC3-II) to the inactive form (LC-I) was determined by Immunoblot. The conjugation of LC3-II from LC3-I is an important step for autophagosome formation. The abundance of LC3-II is increased when the autophagic flux is enhanced. Autophagy was quantified in cells stimulated with and without STSH, and additionally cells were treated or not with the autophagy inhibitor chloroquine (30 μM; Enzo Life Sciences, Farmingdale, NY, USA). Chloroquine disrupts the autophagic flux by inhibiting the fusion of autophagosomes with lysosomes and therefore the number of autophagosomes increases over time. PDL cells where collected by scraping in ice-cold PBS after STSH application for 4 h in the experimental group while untreated cells served as control. After centrifugation, protein lysates were prepared using mechanical disruption in lysis buffer (24 Mm Tris-Cl pH 7.6, 150 mM NaCl, 1% Nonidet P40, 1% Sodium Deoxycholate, 0.1% SDS) plus protease/phosphatase inhibitor cocktail (Halt, Thermo Fisher Scientific, Waltham, USA) boiling at 95 °C for 5 min and clearing by centrifugation (15 min full speed, 4 °C). For immunoblotting, membranes were blocked overnight at 4 °C with 5% (*w*/*v*) non-fat milk in TBS-T (10 mM Tris, pH 7.5, 100 mM NaCl, and 0.05% Tween-20). Anti-LC3B (D11, LC3-II-specific, rabbit; 1:1000, Cell Signaling Technology, 3868) was used at room temperature for 2 h. Horseradish peroxidase (HRP) — coupled Goat Anti-Rabbit IgG-HRP Conjugate (BioRad, 170–6515) served as secondary antibody. Protein loading was controlled by GAPDH (ms-anti-GAPDH IgG, 1:1000, Santa Cruz Biotechnology, Dallas, USA). Visualization of immunoreactive proteins was conducted with chemiluminescence (Amersham Chemiluminescence Kit, GE Healthcare Life Sciences, Freiburg, Germany) and exposure to X-ray films (Agfa, Mortsel, Belgium). Densitometrical analysis was performed with the freely available image-processing software ImageJ 1.43 (https://imagej.nih.gov/ij/).

Autophagosomes were stained using the Cyto-ID® Autophagy Detection Kit (Enzo Life Sciences, #ENZ-51031). The Cyto-ID® Green Detection Reagent accumulates specifically in autophagosomes in pH dependent manner. The staining procedure was conducted according to the manufacturer's instructions and comprised a positive control with the autophagy inducer rapamycin (provided with the kit). Unstained cells served as negative control. In brief, cells of two donors were stimulated or not for 4 h with STSL, STSH, or rapamycin (500 nM). Cells were washed, collected by trypsinization, and incubated with the Cyto-ID® Green Detection Reagent for 30 min at room temperature. Flow cytometry was performed with the FITC Filter (530/30 green) of the blue laser of a BD FACSCalibur (BD Biosciences, Franklin Lakes, USA) and analyzed with the FlowJo Software (BD Biosciences).

Cell death detection

Autophagy often precedes cell death (Mariño et al. 2014). In order to quantify cell death, the amount of cytoplasmic histone-associated DNA fragmentation on the elastic membranes and in cell supernatants was measured. PDL cells of three donors were exposed for 4 h or 24 h to STSL, STSH, rapamycin (500 nM), chloroquine (30 μM, Enzo Life Sciences, an inhibitor of the autophagic flux) or left untreated, and were analyzed with a commercially available enzyme-linked immunosorbent assay (ELISA) kit (Cell Death Detection ELISA^{PLUS}, Roche Diagnostics, Mannheim, Germany) according to the manufacturer's protocol. Final absorbance was determined with a microplate reader (PowerWave x, BioTek Instruments, Winooski, VT, USA) at 405 nm. Data were normalized to total protein concentration by BCA assay (Pierce™ BCA Protein Assay Kit; Thermo Fisher Scientific). Furthermore, the commercially available TUNEL assay (ApoDirekt In Situ DNA Fragmentation Assay Kit, BioVision, Milpitas, CA, USA) was used to determine dead cells on the elastic membrane. PDL fibroblasts of three donors were stimulated as described above and stained with the TUNEL reagent as recommended by the manufacturer. Standardized imaging was conducted with the integrated digital 5-MP CMOS camera of the ZOE™ Fluorescent Cell Imager (Bio-Rad).

Statistical analysis

For statistics, the IBM SPSS Statistics software (Version 22, IBM SPSS, Chicago, IL, USA) was used. Quantitative data are presented as mean and standard deviation (SD). With the exception of the PrimePCRTM Assays, all experiments were performed in triplicate and reproduced at least twice. For statistical comparisons between groups the Kruskal Wallis test followed by the post-hoc Dunnett's tests was used for multiple comparisons. Differences between groups were considered significant at $p < 0.05$. All data are presented as mean±SEM.

Results

Effects of biomechanical loading on autophagy-related target genes

The effects of low and high magnitudes of biomechanical loading on the gene expression of targets known to be involved in autophagy regulation were examined. Static tensile strain of both magnitudes caused gene expression changes on multiple autophagy-associated targets as analyzed by PrimePCR™ Assay (Tables 1 and 2). Stimulation of PDL fibroblasts by both magnitudes of biomechanical loading led to a regulation of B cell lymphoma 2 (BCL2), phosphoinositide-3-kinase, catalytic, gamma polypeptide (PIK3CG), and sequestosome 1 (SQSTM1). Overall, STSH had regulatory effects on more autophagy-associated genes than STSL. The differential gene regulation events due to the various magnitudes of biomechanical loading are visualized in a Venn diagram (Fig. 1a). The regulations of individual genes are shown in Tables 1 and 2. Additionally, an Ingenuity Pathway Analysis (IPA)® (Qiagen) was conducted to create an impression of the complexity of the gene networks regulated by STSL and STSH. The gene network of targets regulated by STSL and STSH were based on information from the Ingenuity Pathways Knowledge Base. The analysis shows that many signaling pathways were activated, including cellular function and maintenance pathways as well as cell death and survival pathways (Fig. 1b, c).

Targets with a fold-change of > 2 where further analyzed by RT-PCR after stimulation with STSL or STSH for 4 h and 24 h (Fig. 2 and Fig. 3). Molecules of two important autophagy regulating systems are shown in Fig. 2: the ubiquitin-like protein conjugation systems (LC3 system), which leads to the completion of LC3-II as a functional part of the autophagosomal membrane and comprises ATG4, ATG7, and ATG10, together with molecules that are involved in beclin-1 activation including BCL2, BH3-interacting domain death agonist (BID), and death-associated protein kinase 1 (DAPK1).

A 24-h stimulation with STSH caused a significant downregulation of ATG4C ($p = 0.001$), ATG7 ($p < 0.001$), and ATG10 ($p = 0.002$) while STSL had no significant effect on the ATGs mRNA expressions. Interestingly, following 4 h of stimulation with STSH, mRNA expression of ATG4C was significantly decreased ($p = 0.032$) while STSL stimulation led to a significant reduction of ATG7 ($p = 0.002$) and ATG10 ($p = 0.02$) expressions (Fig. 2a–c).

At 24 h, BCL2 mRNA expression was significantly downregulated by STSH ($p = 0.009$), while STSL had no significant effects. After 4 h of stimulation, BCL2 mRNA expression was reduced by STSL and STSH ($p = 0.007$ and $p = 0.003$). On the other hand, BID, a competitive inhibitor of BCL2 interactions with beclin-1, was not significantly regulated by STSH stimulation but significantly enhanced by STSL at 24 h ($p = 0.003$). After 4 h of stimulation, BID was significantly reduced by STSL ($p = 0.04$). DAPK1 mRNA expression was significantly downregulated by static tensile strain of both magnitudes after 24 h ($p < 0.001$) but it was not significantly altered by static tensile strain after 4 h of stimulation (Fig. 2d–e).

Furthermore, STSH stimulation for 24 h decreased the expression of alpha-synuclein (SCNA) ($p < 0.05$). Stimulation for 4 h STSH increased significantly tumor suppressor protein

Table 1 Regulation of autophagy-associated genes by static tensile strain of low magnitude (STSL) at 1 day as analyzed with a specific PrimePCR™ assay

Target gene	Control (normalized expression)	STSL (normalized expression)	Regulation of expression (fold of control)
CXCR4	0.00397	0.00719	1.80844
SQSTM1	9.20715	15.45787	1.67890
HGS	0.02725	0.04406	1.61706
TGM2	0.01293	0.02062	1.59486
RGS19	0.00026	0.00015	− 1.69912
BCL2	0.00611	0.00284	− 2.14797
PIK3CG	0.00020	0.00001	− 20.01368

RT-PCR was conducted with pooled cDNA of the three donors. Data normalization was carried with three reference genes (glyceraldehyde-3-phosphate dehydrogenase, hypoxanthine phosphoribosyltransferase 1, TATA box binding protein). Targets with a regulation of more than 1.5-fold were chemokine (C-X-C motif) receptor 4 (CXCR4), sequestosome 1 (SQSTM1), hepatocyte growth factor-regulated tyrosine kinase substrate (HGS), transglutaminase 2 (TGM2), regulator of G protein signaling 19 (RGS19), B cell lymphoma 2 (BCL2) and phosphoinositide-3-kinase, and catalytic, gamma polypeptide (PIK3CG)

p53 (TP53) ($p = 0.005$) and decreased significantly UV radiation resistance associated gene (UVRAG) mRNA expression ($p = 0.008$). STSL led to a reduced UVRAG gene expression after 4 h ($p < 0.001$) (Fig. 3a–d).

Table 2 Regulation of autophagy-associated genes by static tensile strain of high magnitude (STSH) at 1 day as analyzed with a specific PrimePCR™ assay

Target gene	Control (normalized expression)	STSH (normalized expression)	Regulation of expression (fold of control)
BCL2	0.00611	0.01108	1.81315
ATG16L2	0.00629	0.01102	1.75256
ATG4D	0.09711	0.16869	1.73699
SQSTM1	9.20715	14.10767	1.53225
CASP8	0.04188	0.02785	− 1.50409
CTSS	0.03037	0.01999	− 1.51881
AMBRA1	0.01123	0.00728	− 1.54184
GAA	0.02066	0.01257	− 1.64333
APP	1.00479	0.59565	− 1.68688
RB1	0.07449	0.04398	− 1.69368
ESR1	0.00900	0.00518	− 1.73688
PIK3R4	0.05640	0.03117	− 1.80933
SNCA	0.03178	0.01586	− 2.00294
UVRAG	0.03268	0.01582	− 2.06529
ATG7	0.06851	0.03256	− 2.10427
TP53	0.34039	0.15071	− 2.25864
DAPK1	0.00440	0.00187	− 2.35025
BID	0.58386	0.24139	− 2.41874
ATG4C	0.02830	0.01088	− 2.60137
ATG10	0.07943	0.02549	− 3.11606
PIK3CG	0.00020	0.00004	− 4.56672

RT-PCR was conducted with pooled cDNA of the three donors. Data normalization was carried with three reference genes (glyceraldehyde-3-phosphate dehydrogenase, hypoxanthine phosphoribosyltransferase 1, TATA box binding protein). Targets with a regulation of more than 1.5-fold were chemokine B cell lymphoma 2 (BCL2), ATG16 autophagy related 16-like 2 (ATG16L2), ATG4 autophagy related 4 homolog D (ATG4D), sequestosome 1 (SQSTM1), caspase 8, apoptosis-related cysteine peptidase (CASP8), cathepsin S (CTSS), autophagy/beclin-1 regulator 1 (AMBRA1), glucosidase, alpha; acid (GAA), amyloid beta precursor protein (APP), retinoblastoma 1 (RB1), eukaryotic translation initiation factor 4 gamma 1 (ESR1), phosphoinositide-3-kinase, regulatory subunit 4 (PIK3R4), synuclein, alpha (SNCA), UV radiation resistance associated gene (UVRAG), autophagy related 7 (ATG7), tumor protein p53 (TP53), death-associated protein kinase 1 (DAPK1), BH3 interacting domain death agonist (BID), autophagy related 4 homolog C (ATG4C), autophagy related 10 (ATG10) and phosphoinositide-3-kinase, catalytic, and gamma polypeptide (PIK3CG)

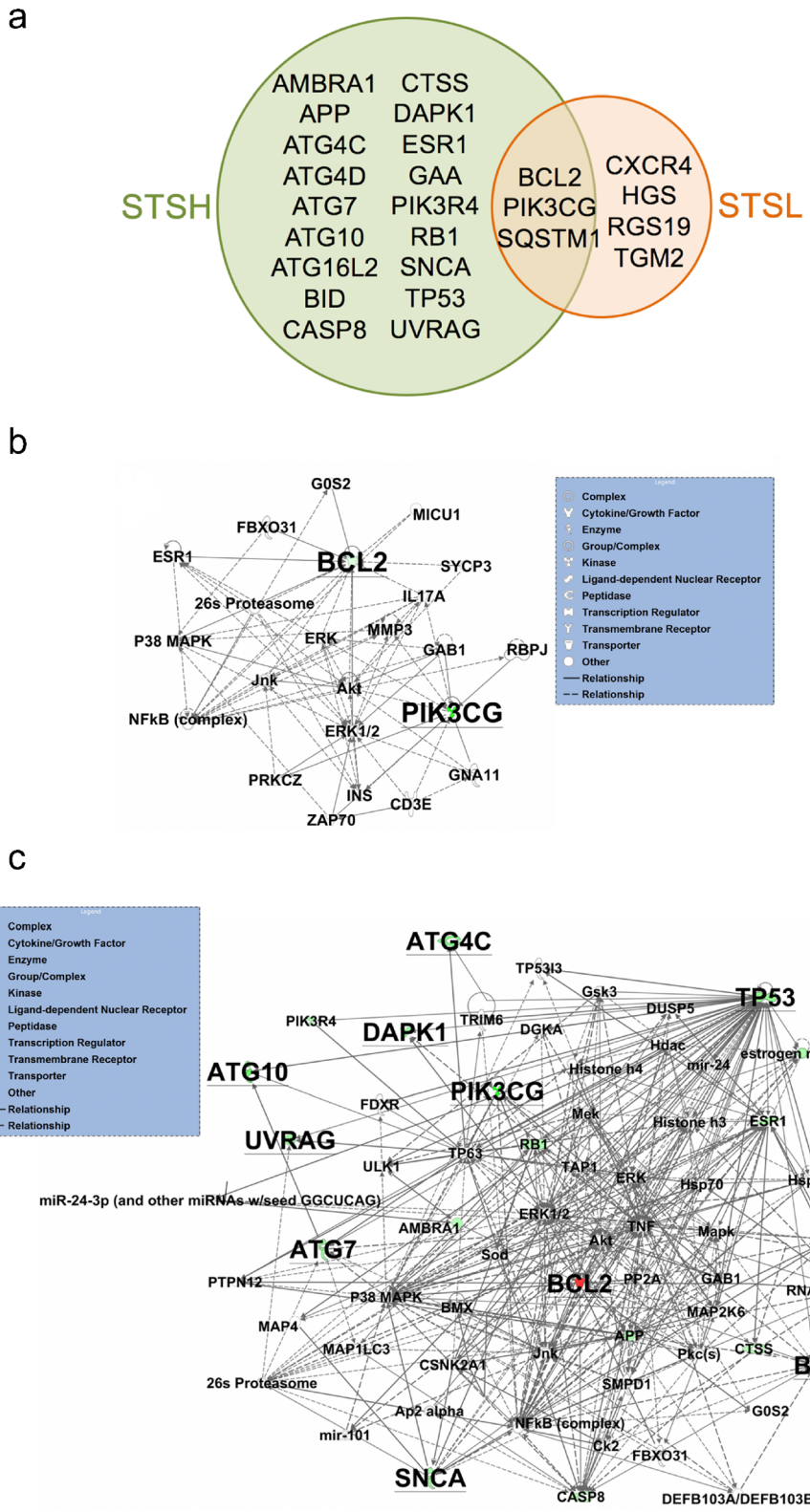

Fig. 1 **a** Venn diagram visualizing the differing gene regulations due to the varying amounts of biomechanical loading. **b**, **c** Ingenuity Pathway Analysis (IPA)® (Qiagen) based on information from the Ingenuity Pathways Knowledge Base. The gene network shows targets regulated by STSL and STSH, respectively. A red symbol indicates upregulation while a green symbol indicates downregulation

Stimulation of autophagy by static tensile strain

In order to measure autophagy regulation by static tensile strain in PDL fibroblasts, immunoblotting for LC3 abundance and conjugation was performed after 4 h of stimulation with STSH (Fig. 4a, b). STSH stimulation led to an increase not only of processed LC3-II but also of LC3-I, which suggests an elevation of the autophagic flux (Fig. 4a, b). The same effect

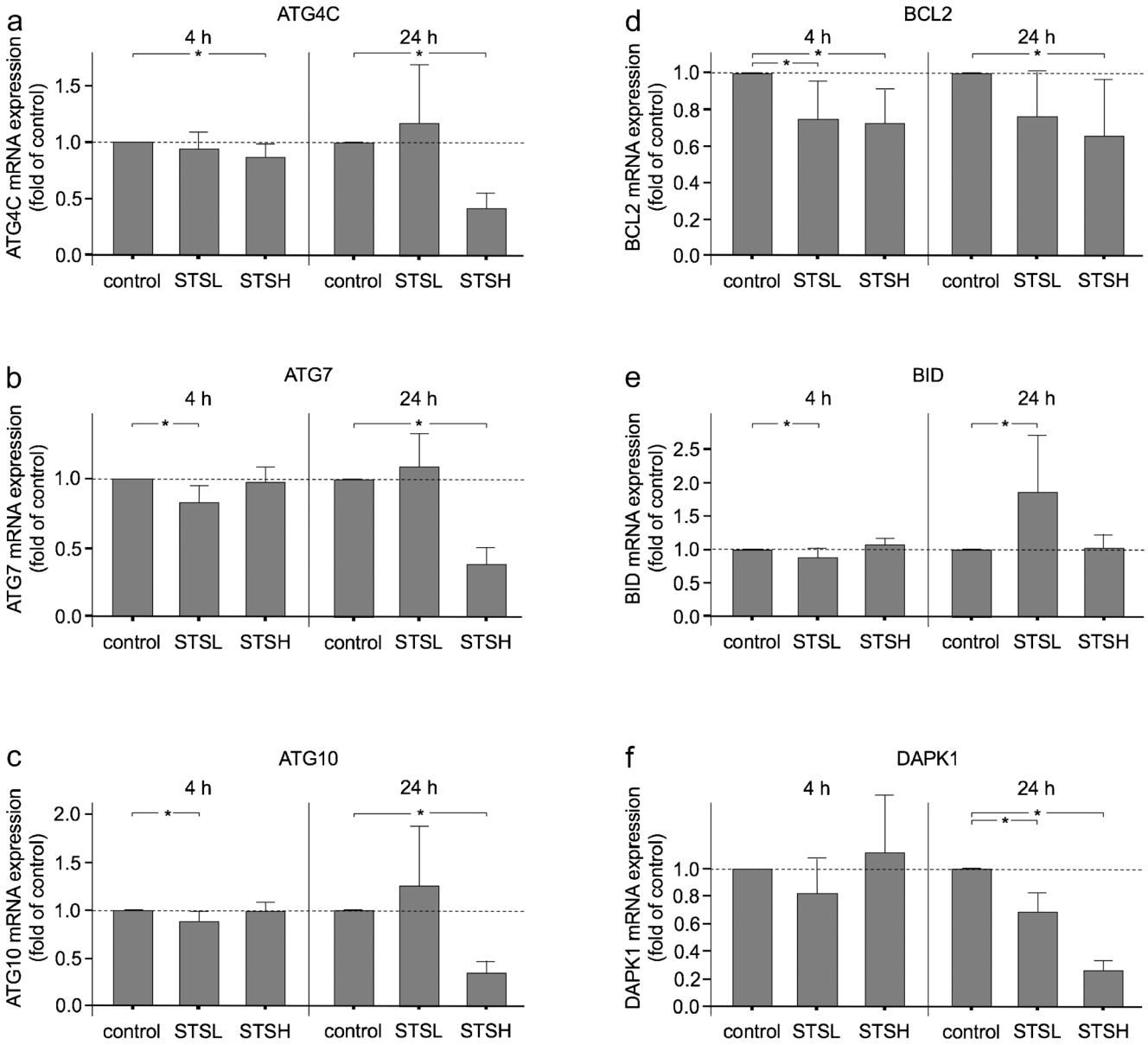

Fig. 2 **a**–**f** Effects of STSL and STSH on mRNA expression of ATG4C, ATG7, ATG10, BCL2, BID, and DPAK1 at 4 h and 24 days. Untreated cells served as control. Mean ± SEM ($n = 9$ replicates derived from three donors); * significant ($p < 0.05$) difference between groups

was observed after inhibition of the autophagic flux with chloroquine. After stimulation with STSH and chloroquine, an accumulation of processed LC3-II and LC3-I was determined as compared to stimulation with chloroquine alone. Stimulation with choloroquine leads to a disruption of the autophagic flux and causes thereby an accumulation of autophagosomes over time. As expected, a greater amount of LC3-I and LC3-II after treatment with choloroquine as compared to cells without inhibitor treatment was shown by immunoblotting (Fig. 4a, b).

Additionally, autophagy regulation was determined by FACS analysis after control, STSL, STSH, and rapamycin treatment for 4 h (Fig. 4c, d). The fluorescence intensity of cells treated with STSH and rapamycin was significantly increased ($p = 0.023$ and $p = 0.002$), which indicated a higher incidence of autophagosomes and therefore an enhancement of the autophagic flux. STSL treatment on the other hand did not change the fluorescence intensity significantly, which suggests a gradual response of autophagy to static tensile strain (Fig. 4d).

Stimulation of cell death by static tensile strain

In order to take the continuous and complex interplay between autophagy and cell death into account, cell death was evaluated in PDL fibroblasts after treatment with STSL, STSH, rapamycin, and chloroquine. As a marker for cell death,

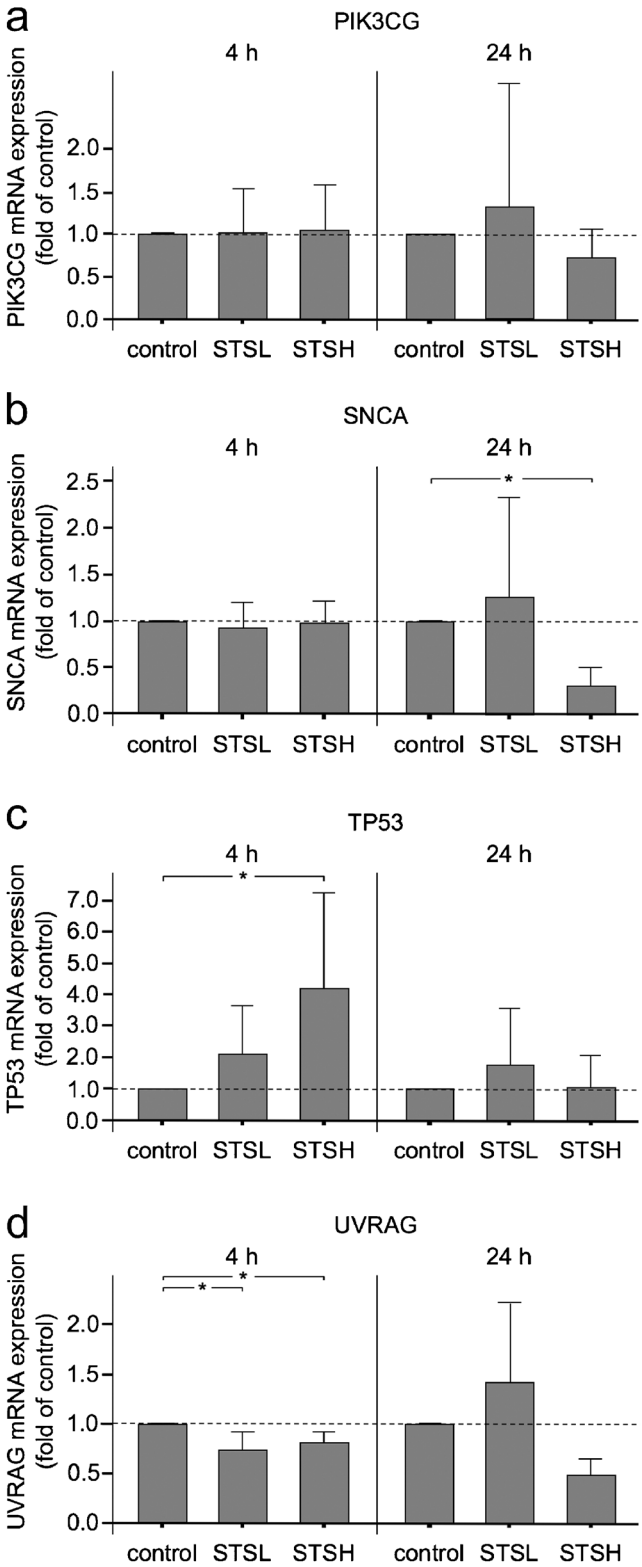

Fig. 3 **a**–**d** Effects of STSL and STSH on mRNA expression of PIK3CG, SNCA, TP53, and UVRAG at 4 h and 24 days. Untreated cells served as control. Mean ± SEM ($n = 9$ replicates derived from three donors); * significant ($p < 0.05$) difference between groups.

DNA fragmentation was measured on the elastic membranes (Fig. 5a–d) as well as in cell supernatants (Fig. 5e, f).

STSL treatment significantly reduced DNA fragmentation as determined on membranes and in supernatants after 4 h ($p = 0.001$ and $p < 0.001$) as well as in supernatants after 24 h ($p = 0.03$). Therefore, STSL seems to have cell protective properties. On the other hand, chloroquine treatment led to a significant increase in cell death of attached cells at both time points ($p < 0.001$) as well as in cell supernatants after 24 h ($p < 0.001$). STSH and rapamycin treatment increased the number of dead cells on the elastic membranes after 24 h ($p = 0.046$ and $p = 0.001$) but did not alter DNA fragmentation in supernatants as compared to control (Fig. 5c–f).

Discussion

The present study provides novel evidence that autophagy is regulated by static tensile strain in PDL fibroblasts. The autophagic flux seems to be enhanced by high magnitudes of static tensile strain while low magnitudes of static tensile strain had no significant effect on the amount of autophagosome formation. Interestingly, both magnitudes of strain had regulatory effects on mRNA expression of autophagy-associated targets, but stimulation with STSH induced mRNA expression changes of more autophagy-associated targets than STSL. Taken together, our results suggest a gradual response of autophagy to static tensile strain in human PDL fibroblasts. Furthermore, autophagy seems to be an important mechanism for cell homeostasis in PDL fibroblasts as autophagy inhibition led to cell death in our experiments. Low magnitudes of tensile strain, on the other hand, seem to have cell protective properties.

Our findings show a strain-dependent regulation of different autophagy-associated targets. King and coworkers demonstrated a graduated response of autophagy to mechanical stimulation (King et al. 2011). In their study, they used pressure to stimulate MDA-MB-231 cells (King et al. 2011). However, King hypothesized that autophagy was induced by poor adaptation to an altered physical environment and that other kinds of physical challenges also regulate autophagy (King 2012). Our results fit very well to King's hypothesis as autophagy regulation in PDL fibroblasts was induced by tensile strain in our study.

We started with an unbiased approach to analyze autophagy-associated targets and their regulation by different magnitudes of static tensile strain. Autophagy regulation is a very dynamic process and post-translational modifications allow for rapid adaption. However, autophagy, as many adaptive stress responses, develops along a biphasic kinetics, and there is a second phase of autophagy regulation which takes place on transcriptional level. In order to preserve or re-establish homeostasis for more permanent changes of

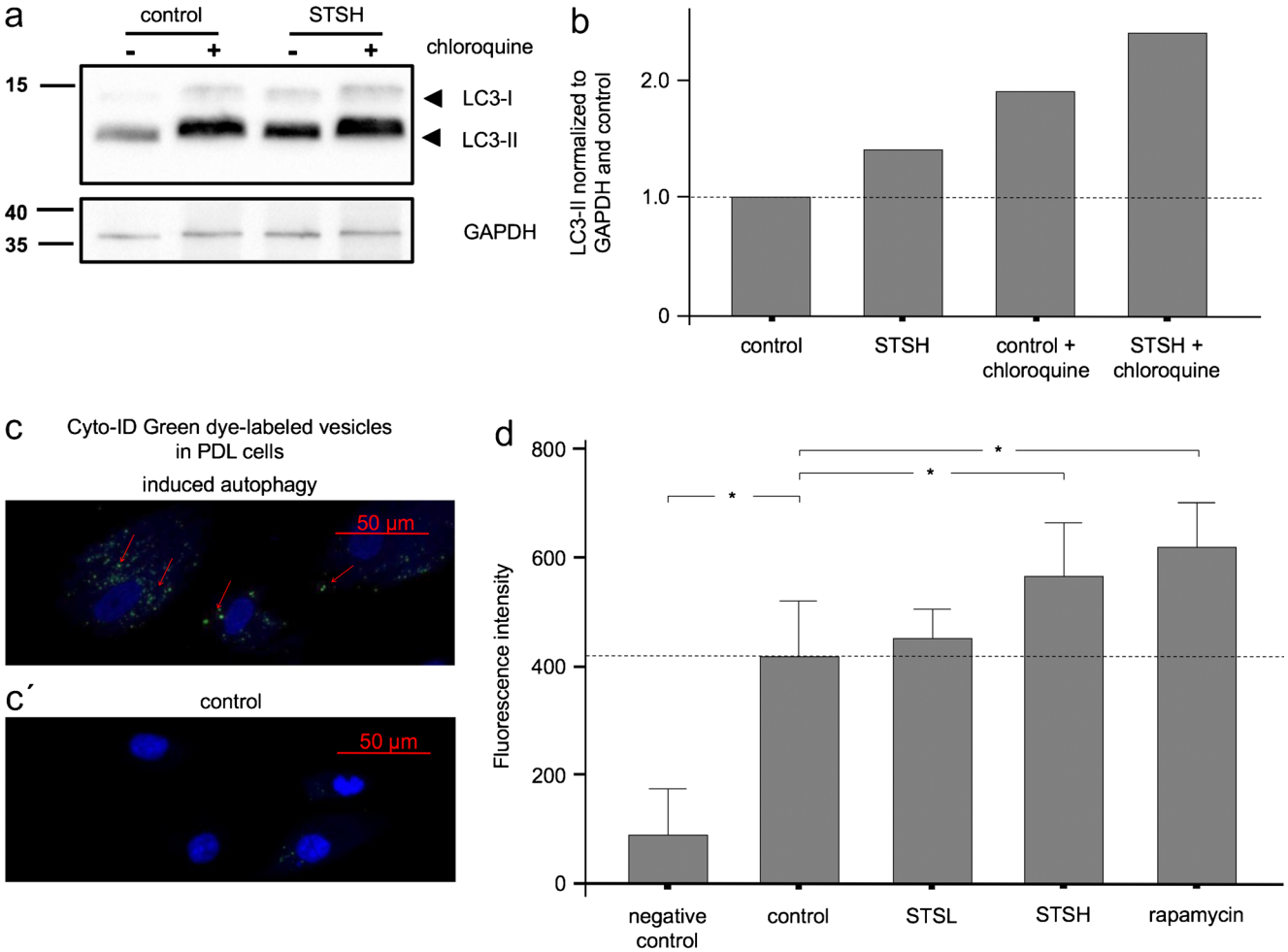

Fig. 4 **a** Effects of 4-h treatment with STSH in combination or not with chloroquine, an inhibitor of the autophagic flux, on the abundance of LC3-I and LC3-II as shown by immunoblot. Untreated cells served as control. A representative image of one donor is shown. **b** Results of the semi-quantitative analysis performed by ImageJ software to determine LC3-II/LC3-I ratio. (**c**, **c′**) Visualization of the effect of 4 h rapamycin treatment (**c**) in comparison to untreated controls (**c′**) after autophagosome staining in PDL fibroblasts with the Cyto-ID® Autophagy Detection Kit as shown by fluorescence microscopy. **d** FACS analysis of autophagosomes in PDL fibroblasts stained with the Cyto-ID® Autophagy Detection Kit. Untreated cells served as negative control. Prior to staining, cells were stimulated with STSL, STSH, rapamycin or no treatment for 4 h. Mean ± SEM ($n = 6$ replicates derived from two donors); * significant ($p < 0.05$) difference between groups

environment, specific transcription factors are activated and gene expression changes are induced (Pietrocola et al. 2013). Therefore, we chose 24 h of stimulation as timepoint for our PrimePCR™ Assay.

On the basis of our array findings, we selected targets for further investigation. Gene expression was determined after 4 h and 24 h. Interestingly, gene expression changes after 4 h were mostly induced by STSL but after 24 h changes were mostly induced by STSH. Two important autophagy-regulating systems were found to be influenced by biomechanical loading after 24 h.

One system controls the conjugation of LC3 which is an essential element of the autophagosomal membrane. ATG4 cleaves LC3 at its carboxyl terminus. The ubiquitin-activating enzyme, ATG7, catalyzes the first step in the ubiquitination reaction enzyme for LC3 and also for ATG12. The second protein, ATG10, acts as an ubiquitin carrier in the further conjugation of ATG12, which in turn is needed to complete the last step of the LC3 conjugation (Mariño et al. 2014). The components of this system (ATG4C, ATG7, and ATG10) were all downregulated by STSH after 24 h of stimulation indicating transcriptional a downregulation of autophagy.

The second system is involved in autophagy regulation through beclin-1 activation. The lipid kinase vacuolar protein sorting 34 (VPS34)-beclin-1 complex orchestrates the assembly of the ATGs at the phagophore assembly site and initiates the elongation of the isolation membrane (Lippai and Szatmári 2017). Beclin-1 is usually inactivated by anti-apoptotic proteins of the BCL2 family. BID, on the other hand, promotes autophagy by enabling beclin-1 to dissociate from BCL2. BID also activates the intrinsic pathway of apoptosis (Mariño et al. 2014). Therefore, a downregulation of BCL2 by 24 h of STSH

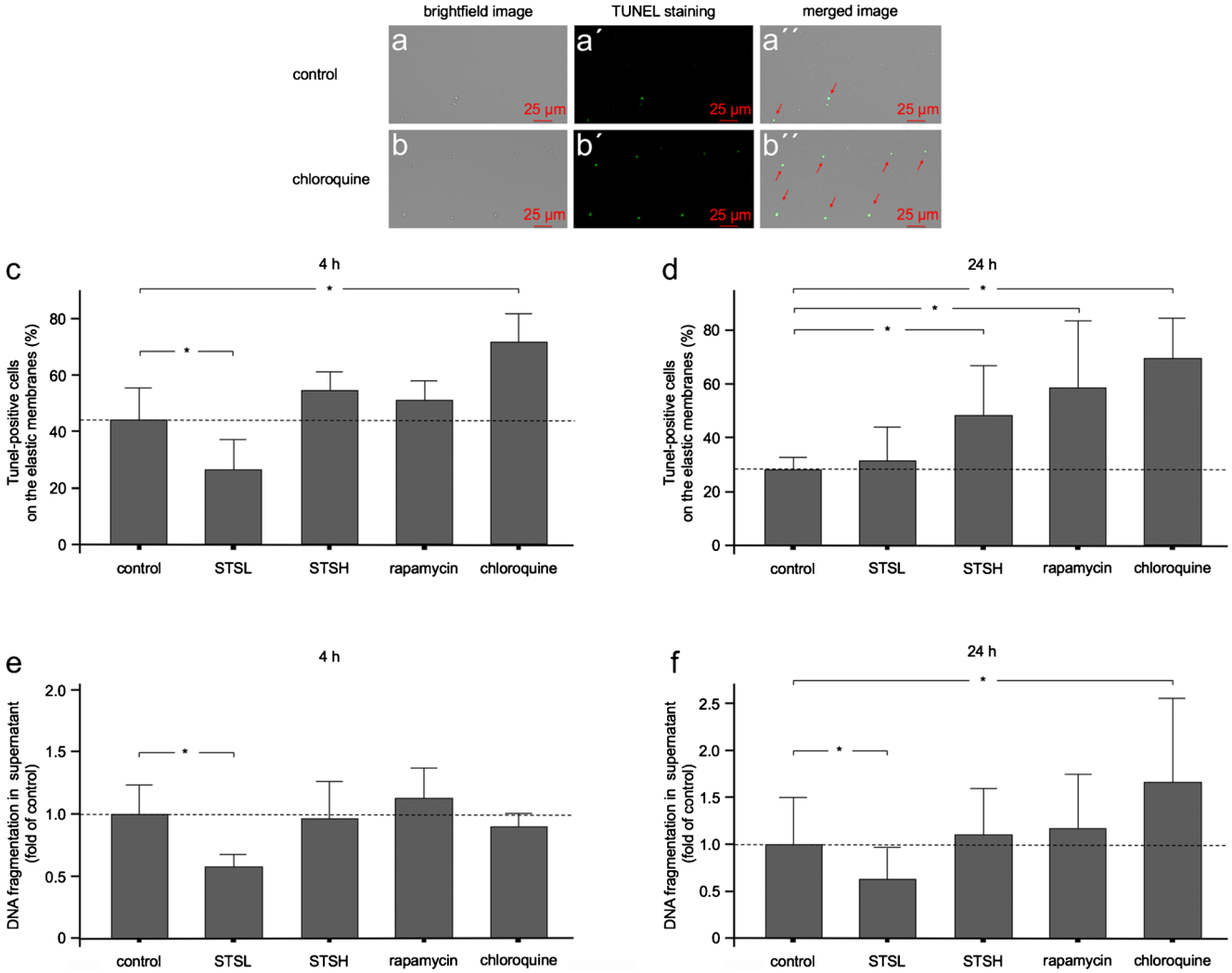

Fig. 5 **a**, **b** Representative image of TUNEL staining in PDL fibroblasts with the ApoDirekt In Situ DNA Fragmentation Assay Kit. Control cells (**a**, **a′**, **a″**) are shown in comparison with cells after 4 h of chloroquine treatment (**b**, **b′**, **b″**). Arrows indicate examples of TUNEL positive cells. **c**, **d** Effects of PDL fibroblast stimulation with STSL, STSH, autophagy inducer rapamycin and autophagy inhibitor chloroquine on Tunel-positive cells on the elastic membrane after 4 h and 24 h, respectively. Untreated cells served as control. Mean ± SEM ($n = 9$ replicates derived from three donors); * significant ($p < 0.05$) difference between groups (**e**, **f**). Effects of PDL fibroblast stimulation with STSL, STSH, autophagy inducer rapamycin, autophagy inhibitor chloroquine on DNA fragmentation in supernatant after 4 h and 24 h, respectively, as analyzed by Cell Death Detection ELISA^{PLUS}. Untreated cells served as control. Mean ± SEM ($n = 9$ replicates derived from three donors); * significant ($p < 0.05$) difference between groups

stimulation indicates not only an induction of autophagy but also of apoptosis. BID upregulation by STSL may promote autophagy by the disruption of beclin-1 and BCL2. DAPK1 activates autophagy in two ways, firstly by phosphorylating beclin-1 and thereby interrupting its interaction with BCL2 and by activating a second kinase, which phosphorylates and activates VPS34 (Mariño et al. 2014). Therefore, a downregulation of DAPK1 by STSL and STSH after 24 h of stimulation indicates a transcriptional downregulation of autophagy.

Taken together, after 24 h of STSH stimulation, gene expression changes are mostly in favor of autophagy downregulation in PDL fibroblasts, with the exception of BCL2 downregulation. However, BCL2 downregulation may also be pro-apoptotic. BID upregulation after 24 h of STSL could affect the PDL fibroblasts in a pro-apoptotic and pro-autophagic manner while DAPK1 downregulation indicates a downregulation of autophagy in PDL fibroblasts. The cellular mechanisms responsible for autophagy regulation following mechanical stimulation in PDL fibroblasts are not fully understood so far and should be investigated in future studies. Many pathways and molecules involved in transduction of mechanical signals including calcium, inositol (1, 4, 5)-trisphosphate, nitric oxide, Ras, Src, focal adhesion kinase, and mitogen-activated protein kinase, have also been shown to regulate autophagy (King 2012). However, the systems found to be regulated by mechanical stimulation in our study LC3-II conjugation and on beclin-1 activation could be an important part of autophagy regulation in PDL-cells.

Besides the two autophagy-regulating systems, other genes with a fold-change of > 2 were also selected for further investigation. PIK3CG which was pronouncedly regulated according to the PrimePCR™ Assay could not be confirmed by RT-PCR. This may be due to the very high threshold cycle and the low normalized expression, making gene expression changes very susceptible to fluctuation. Some other discrepancies between the array results and the further validation of gene expression changes were found. Validation and array discrepancies may be due to pooling effects in the array. Furthermore, in the PrimePCR™ Assay normalization was done, as instructed by the manufacturer, to the three reference genes GAPDH, and HPRT1 and TRP. In the following assessment of gene expression changes only GAPDH was applied for normalization. The employment of GAPDH as a reference gene in PDL cells under mechanical stimulation is currently under discussion, considering a recent study which investigated the stability of reference genes in PDL cells under compression. Under the conditions of this study Peptidylprolyl Isomerase A and ribosomal protein L22 showed higher expression stabilities than GAPDH and might therefore be more suitable as reference genes in PDL cells under compression (Kirschneck et al. 2017). Nevertheless, we chose GAPDH as housekeeping gene in our study to provide comparable results to previous studies (Memmert et al. 2017; Memmert et al. 2018). However, future studies about the stability of reference genes in PDL cells under strain are needed.

In our study, we did not only assess the regulation of autophagy-associated genes but we attempted to measure autophagy by analyzing LC3-II abundance and conjugation as well as autophagosome quantification. Autophagy was enhanced by 4 h of STSH stimulation. STSL stimulation for 4 h did not increase the amount of autophagosome formation significantly. It has been reported that autophagy is induced by the environmental change itself rather than the absolute stimulus. A prolonged mechanical stimulus initially enhanced autophagy, but once the cell has adapted by alteration of its cytoskeleton autophagy is reduced to its initial level (King 2012). In a dynamic situation, on the other hand, autophagy has been shown to stay elevated for 24 h (Chen et al. 2015). However, if the dynamic stimulus becomes a permanent situation, autophagy has been shown to be reduced again (Xu et al. 2014). Therefore, our findings fit very well in the current literature as we also observed that autophagy was enhanced by 4 h of mechanical stimulation. Additionally, an increased number of autophagosomes was determined in cells after pressure application, and this reaction was graduated in response to the amount of applied pressure (King et al. 2011). Our findings also suggest that autophagy responds gradually to mechanical stimulation as only STSH was able to increase autophagy significantly and STSL stimulation did not lead to significant changes, but showed a trend towards upregulation.

Some difficulties arise in autophagy analysis, because autophagy is a highly dynamic process (Klionsky et al. 2016). Therefore, we used autophagy markers such as LC3-II for autophagy quantification in a combination with chloroquine treatment, which arrests the autophagic flux, inhibits the degradation of autophagosomes, and allows their accumulation over time. We concluded that STSH did increase LC3-I and LC3-II as a result of enhanced autophagy and not of decreased degradation. According experiments with chloroquine were performed in advance to the FACS analysis (results not shown). LC3 is the most frequently used protein to monitor autophagy. However, LC3-II is also part of membranes of non-autophagic structures, as apoptotic phagosome membranes or secretory lysosomes (Klionsky et al. 2016). Therefore, it is recommended to confirm autophagy analysis by another method (Klionsky et al. 2016). In our study, we chose the LC3-independent Cyto-ID assay to provide a numeric readout that correlates with autophagy-associated vacuoles (Guo et al. 2015).

As a mechanism of adaption, a key function of autophagy is damage limitation but many stress pathways sequentially initiate autophagy and apoptosis within the same cell (Mariño et al. 2014). Therefore, cell death was assessed in PDL fibroblasts after treatment with STSL, STSH, rapamycin, and chloroquine. Our findings imply that STSL has cell protective properties. STSH on the other hand increased the amount of dead cells on the stretched membrane after 24 h. Furthermore, autophagy inhibitor choloroquine induced cell death after 24 h of stimulation. This finding emphasizes the importance of autophagy for cell homeostasis in PDL fibroblasts.

Autophagy is a mechanism which secures cell survival under biomechanical loading and generally blocks the induction of apoptosis. However, when the mechanical stimulus exceeds a certain amount in duration or magnitude, the excessive autophagy can lead to cell death via crosstalk with apoptosis pathways (Ma et al. 2013; Mariño et al. 2014). King stated that mechanical activation of autophagy under normal physiological forces may help to suppress cell death with the help of autophagy (King 2012). On the other hand, other studies imply that autophagy inhibitors reduce cell death after mechanical stimulation (Chen et al. 2015). Autophagy does not only induce apoptosis under certain conditions but also initiates an autophagic cell death as a consequence of stress overload (Ma et al. 2013; Mariño et al. 2014). Overall, our results fit very well to the recent literature. They suggest that low forces suppress cell death via a moderate induction of autophagy. A high magnitude of strain induces autophagy after 4 h, but when the stimulus exceeds a certain duration the mechanical overload enhances the number of dead cells.

Measurement of cell death was based on the principle of measuring DNA fragmentation, which is characteristic of the apoptotic process. In this study, antibodies directed against

fragmented DNA and histone-associated DNA fragments, respectively, were used which mark the very late state of apoptosis. To analyze early apoptotic changes, other methods would have been more appropriate. Furthermore, other forms of cell death like autophagic cell death would also be detected by the methods used in our study. Therefore, it was not possible to distinguish autophagic cell death and apoptosis in this study. It was the aim of this study to determine the cell fate of the stimulated cells. In order to include all stimulated cells in our measurement, we analyzed cells on elastic membranes but also determined DNA fragmentation in supernatants because dead cells detach from elastic membranes.

Physiologically, the PDL is exposed to various types of biomechanical stress, e.g., through chewing movements. Within the limitations for clinical transferability of the results of an in vitro study, we attempted to improve generalizability of our results by using force magnitudes, which were found to be realistic in comparison to the strain subjected to the periodontal ligament in the course of orthodontic tooth movement, by chewing or grinding (Natali et al. 2004). In vivo biomechanical stress leads to adaptation processes in the entire periodontium, which are mainly orchestrated by PDL fibroblasts. PDL fibroblasts represent an important point of action for any application of force in the periodontium. Therefore, we chose to use PDL fibroblasts in our study. However, autophagy regulation in other cells of the periodontium, e.g., cells involved in bone turnover like osteoclasts and osteoblasts, would be an interesting subject for a future research. We demonstrated that STSL reduced cell death. These results are in line with earlier studies which suggested biomechanical stimulation to be an important factor in PDL fibroblast homeostasis. PDL fibroblasts were subjected to low magnitudes of biomechanical loading and subsequently gene expression of anti-apoptotic pathways were induced (Deschner et al. 2012). Overload on the other hand induced cell death in PDL fibroblasts (Wu et al. 2016; Xu et al. 2011; Zhao et al. 2017). Our results not only confirm but also expand earlier findings as they suggest that autophagy might be involved in PDL fibroblast homeostasis. We demonstrated that autophagy induction and even more autophagy inhibition can induce cell death in PDL fibroblasts.

Based on our findings in PDL fibroblasts, we hypothesize that autophagy is involved in orthodontic tooth movement. Therefore, our results are in line with findings of Nakamura and coworkers. In their study, they found vacuoles containing various cell organelles by electron-microscopic examination in osteoblasts and fibroblasts in the periodontium of Wistar rats after 24 h of tooth movement. These vacuoles were identified as autophagosomes on the basis of their contents (Nakamura et al. 1984). One major difficulty of in vivo autophagy analysis is that multiple stimuli influence autophagy and therefore it is not possible to focus on one specific stimulus for autophagy induction. Orthodontic tooth movement involves a plethora of stimuli, e.g., oxygen level changes and inflammation (Li et al. 2018). Therefore, defined in vitro studies are required to compliment in vivo studies for a better understanding of the molecular mechanism in autophagy regulation.

Taken together, our findings provide novel insights into autophagy regulation by biomechanical loading in human PDL fibroblasts. Autophagy caused a dose-dependent response to mechanical strain and was upregulated by STSH after 4 h. Additionally, the results of our study imply that autophagy might play a key role in PDL fibroblast homeostasis. Therefore, autophagy might be an important process in orthodontic tooth movement controlling survival and death of PDL fibroblasts depending on the force applied.

Acknowledgments The authors would like to thank Dr. Michaela Rinneburger, Dr. Benedikt Kleineidam, Ms. Ramona Menden, Ms. Silke van Dyck, and Ms. Inka Bay for their valuable support.

Funding statement This study was supported by the Medical Faculty of the University of Bonn, the German Research Foundation (DFG, ME 4798/1-1) and the German Orthodontic Society (DGKFO).

Compliance with ethical standards

Conflict of interest The authors declare that they have no conflict of interest.

Research involving human participants and/or animals All procedures performed in studies involving human participants were in accordance with the ethical standards of the institutional and/or national research committee and with the 1964 Helsinki declaration and its later amendments or comparable ethical standards.

PDL cells were taken after the approval of the Ethics Committee of the University of Bonn was given (#117/15). Patients or their legal guardians provided written informed consent before PDL cells were harvested.

Informed consent Informed consent was obtained from all individual participants included in the study.

References

Basdra EK, Komposch G (1997) Osteoblast-like properties of human periodontal ligament cells: an in vitro analysis. Eur J Orthod 19: 615–621

Chen H, Chen L, Cheng B, Jiang C (2015) Cyclic mechanical stretching induces autophagic cell death in tenofibroblasts through activation of prostaglandin E2 production. Cell Physiol Biochem 36:24–33

Deschner B, Rath B, Jäger A, Deschner J, Denecke B, Memmert S, Götz W (2012) Gene analysis of signal transduction factors and transcription factors in periodontal ligament cells following application of dynamic strain. J Orofac Orthop 73:486–495, 497

Glick D, Barth S, Macleod KF (2010) Autophagy: cellular and molecular mechanisms. J Pathol 221:3–12

Guo S, Liang Y, Murphy SF, Huang A, Shen H, Kelly DF, Sobrado P, Sheng Z (2015) A rapid and high content assay that measures cyto-ID-stained autophagic compartments and estimates autophagy flux with potential clinical applications. Autophagy 11:560–572

Huang WP, Klionsky DJ (2002) Autophagy in yeast: a review of the molecular machinery. Cell Struct Funct 27:409–420

King JS (2012) Mechanical stress meets autophagy: potential implications for physiology and pathology. Trends Mol Med 18:583–588

King JS, Veltman DM, Insall RH (2011) The induction of autophagy by mechanical stress. Autophagy 7:1490–1499

Kirschneck C, Batschkus S, Proff P, Köstler J, Spanier G, Schröder A (2017) Valid gene expression normalization by RT-qPCR in studies on hPDL fibroblasts with focus on orthodontic tooth movement and periodontitis. Sci Rep 7:14751

Klionsky DJ, Abdelmohsen K, Abe A et al (2016) Guidelines for the use and interpretation of assays for monitoring autophagy (3rd edition). Autophagy 12:1–222

Krishnan V, Davidovitch Z, Bahar H (2015) Biological mechanisms of tooth movement, 2nd Edition. Wiley-Blackwell, Chichester

Kroemer G, Mariño G, Levine B (2010) Autophagy and the integrated stress response. Mol Cell 40:280–293

Li M, Khambu B, Zhang H, Kang JH, Chen X, Chen D, Vollmer L, Liu PQ, Vogt A, Yin XM (2013) Suppression of lysosome function induces autophagy via a feedback down-regulation of MTOR complex 1 (MTORC1) activity. J Biol Chem 288:35769–35780

Li Y, Jacox LA, Little SH, Ko CC (2018) Orthodontic tooth movement: the biology and clinical implications. Kaohsiung J Med Sci 34:207–214

Lippai M, Szatmári Z (2017) Autophagy-from molecular mechanisms to clinical relevance. Cell Biol Toxicol 33:145–168

Ma Y, Galluzzi L, Zitvogel L, Kroemer G (2013) Autophagy and cellular immune responses. Immunity 39:211–227

Marchesan JT, Scanlon CS, Soehren S, Matsuo M, Kapila YL (2011) Implications of cultured periodontal ligament cells for the clinical and experimental setting: a review. Arch Oral Biol 56:933–943

Mariño G, Niso-Santano M, Baehrecke EH, Kroemer G (2014) Self-consumption: the interplay of autophagy and apoptosis. Nat Rev Mol Cell Biol 15:81–94

Mariotti A, Cochran DL (1990) Characterization of fibroblasts derived from human periodontal ligament and gingiva. J Periodontol 61:103–111

Memmert S, Damanaki A, Nogueira AVB, Eick S, Nokhbehsaim M, Papadopoulou AK, Till A, Rath B, Jepsen S, Götz W, Piperi C, Basdra EK, Cirelli JA, Jäger A, Deschner J (2017) Role of cathepsin S in periodontal inflammation and infection. Mediat Inflamm 2017:4786170

Memmert S, Nogueira AVB, Damanaki A, Nokhbehsaim M, Eick S, Divnic-Resnik T, Spahr A, Rath-Deschner B, Till A, Götz W, Cirelli JA, Jäger A, Deschner J (2018) Damage-regulated autophagy modulator 1 in oral inflammation and infection. Clin Oral Investig 22:2933–2941

Mizushima N, Komatsu M (2011) Autophagy: renovation of cells and tissues. Cell 147:728–741

Nakamura Y, Hirashita A, Kuwabara Y (1984) The localization of acid phosphatase activity in osteoblasts incident to experimental tooth movement. Acta Histochem Cytochem 17:581–582

Natali AN, Pavan PG, Scarpa C (2004) Numerical analysis of tooth mobility: formulation of a non-linear constitutive law for the periodontal ligament. Dent Mater 20:623–629

Noda T, Ohsumi Y (1998) Tor, a phosphatidylinositol kinase homologue, controls autophagy in yeast. J Biol Chem 273:3963–3966

Pietrocola F, Izzo V, Niso-Santano M, Vacchelli E, Galluzzi L, Maiuri MC, Kroemer G (2013) Regulation of autophagy by stress-responsive transcription factors. Semin Cancer Biol 23:310–322

Salabei JK, Hill BG (2015) Autophagic regulation of smooth muscle cell biology. Redox Biol 4:97–103

Towers CG, Thorburn A (2016) Therapeutic targeting of autophagy. EBioMedicine 14:15–23

Wesselborg S, Stork B (2015) Autophagy signal transduction by ATG proteins: from hierarchies to networks. Cell Mol Life Sci 72:4721–4757

Wu Y, Zhao D, Zhuang J, Zhang F, Xu C (2016) Caspase-8 and Caspase-9 functioned differently at different stages of the cyclic stretch-induced apoptosis in human periodontal ligament cells. PLoS One 11:e0168268

Xu C, Hao Y, Wei B, Ma J, Li J, Huang Q, Zhang F (2011) Apoptotic gene expression by human periodontal ligament cells following cyclic stretch. J Periodontal Res 46:742–748

Xu HG, Yu YF, Zheng Q, Zhang W, Wang CD, Zhao XY, Tong WX, Wang H, Liu P, Zhang XL (2014) Autophagy protects end plate chondrocytes from intermittent cyclic mechanical tension induced calcification. Bone 66:232–239

Zhao D, Wu Y, Xu C, Zhang F (2017) Cyclic-stretch induces apoptosis in human periodontal ligament cells by activation of caspase-5. Arch Oral Biol 73:129–135

Publisher's note Springer Nature remains neutral with regard to jurisdictional claims in published maps and institutional affiliations.